Anomalous Ion Channeling in AlInN/GaN Bilayers: Determination of the Strain State

K. Lorenz,[1,*] N. Franco,[1] E. Alves,[1] I. M. Watson,[2] R. W. Martin,[3] and K. P. O'Donnell[3]

[1]*Instituto Tecnológico e Nuclear, Estrada Nacional 10, 2686-953 Sacavém, Portugal*
[2]*Institute of Photonics, SUPA, University of Strathclyde, Glasgow G4 0NW, United Kingdom*
[3]*Department of Physics, SUPA, University of Strathclyde, Glasgow, G4 0NG, United Kingdom*

Monte Carlo simulations of anomalous ion channeling in near-lattice-matched AlInN/GaN bilayers allow an accurate determination of the strain state of AlInN by Rutherford backscattering or channeling. Although these strain estimates agree well with x-ray diffraction (XRD) results, XRD composition estimates are shown to have limited accuracy, due to a possible deviation from Vegard's law, which we quantify for this alloy. As the InN fraction increases from 13% to 19%, the strain in AlInN films changes from tensile to compressive with lattice matching predicted to occur at $[InN] = 17.1\%$.

An issue of fundamental importance in semiconductor physics continues to be the measurement of strains within multilayer heterostructures. These include strained-layer structures incorporating wide-gap group III nitride semiconductors which have an impressive variety of realized and proposed applications in (opto-) electronic devices [1]. Improved device performance is expected to follow the development of lattice-matched III nitride heterostructures, as a consequence of the elimination of misfit dislocation formation. Although the determination of AlInN structural properties may be made difficult by phase separation during epitaxial growth, driven by a large disparity in cation sizes, the possibility of lattice matching this alloy to GaN makes it an attractive alternative to InGaN and AlGaN for applications in GaN-based devices, e.g., for cladding layers, Bragg mirrors, insulating layers, or as channel layers in field effect transistors [2–4]. The increasing availability of freestanding or bulk GaN substrates underpins the development of AlInN/GaN based devices with low defect densities as an attractive prospect [4].

Ion channeling has proved successful in strain measurements of a wide variety of thin layer semiconductor systems including III-nitrides [5,6]. In the channeling process a particle beam (typically of protons or α particles with energies of 1–2 MeV) is directed along a low-index crystal axis and penetrates deep into the crystal with significantly reduced yield of backscattered particles. A Rutherford Backscattering/Channeling (RBS/C) angular scan is obtained by measuring the backscattering yield in a certain energy window (which corresponds to a certain depth interval in the sample) as a function of angle between the incoming beam and the channeling crystal axis. The width of the channeling dip depends on the value for the critical angle: the maximum incident angle for which particles are steered between atomic rows without undergoing large-angle deviation. Reference [7] gives a detailed description of the channeling technique.

In an AlInN/GaN bilayer the different lattice parameters of the two constituent materials cause a change of the tilt angle (the kink angle $\Delta\theta$) in the interface for atomic rows

and crystal planes that are not perpendicular to the surface, as illustrated in Fig. 1. The kink angle changes when films are strained by pseudomorphic growth. When angular scans are performed along the plane containing the $\langle 0001 \rangle$ and the tilted axis, the minima of the dips for AlInN and GaN will occur at different angles—displaced from each other by $\Delta\theta$. In Fig. 1, $\Delta\theta$ is the real kink angle in the interface, $\Delta\Phi$ is the angular shift caused by strain of the AlInN layer, and $\Delta\alpha$ that between GaN and relaxed AlInN. The tilt angle Φ of the $\langle \bar{2}113 \rangle$ axis towards the $\langle 0001 \rangle$ axis is given by $\tan\Phi = a/c$ ($\tan\Phi = \sqrt{3}a/c$ for the $\langle 10\bar{1}1 \rangle$ axis), so that $\Delta\alpha$ can be determined using the lattice parameters of the GaN-buffer layer ($a = 3.185$ Å, $c = 5.188$ Å) and of relaxed AlInN derived from Vegard's law [8]. $\Delta\Phi$ ($\Delta\Phi = \Delta\theta - \Delta\alpha$) is related to the strain in the layer through the tetragonal distortion given by $\varepsilon_T = \Delta\Phi/(\sin\Phi \cos\Phi)$.

However, in the case of high crystalline quality layers and $\Delta\theta$ comparable to, or smaller than, the critical angle, the steering potential of the lattice is strong enough to bend the beam and keep a fraction of the particles channeled across the interface. These steering effects, also referred to as "anomalous channeling" [9], change the angular yield of the second layer (in our case, the GaN-buffer layer). They will cause the conventional method of measuring

FIG. 1. Illustration to explain the change in tilt in the interface of a $\langle \bar{2}113 \rangle$ axis in strained and relaxed AlInN films on GaN.

strain by RBS/C to fail since the displacement of the angular scans no longer corresponds to the real kink angle.

Accurate determination of the strain in heteroepitaxial layers requires absolute determination of the tilt angles; however, small inaccuracies in the experimental setup have an adverse effect on such measurements. Steering effects are reduced for planar channeling due to the smaller critical angles. However, even "state-of-the-art" nitride films show a reduced crystalline quality for off-normal directions; in our samples dechanneling within the relatively thick AlInN layers is too strong to get reliable measurements by means of planar channeling.

In this Letter, we present an RBS/C study in AlInN/GaN bilayers in which we use Monte Carlo (MC) simulations to fully account for steering effects. The measurement of strain by RBS/C in combination with MC simulations is demonstrated to give excellent agreement with x-ray diffraction (XRD) data but significant differences are revealed in the measured AlInN compositions. This discrepancy can be eliminated by introducing a correction to Vegard's law.

$Al_{1-x}In_xN$ layers with thicknesses of ca. 100 nm were grown by metal organic chemical vapor deposition (MOCVD) on GaN-buffer layers on (0001) sapphire at different set-point growth temperatures. In the following, three samples grown at 800, 820, and 840 °C will be referred to as S800, S820, and S840, respectively. RBS/C measurements were performed with a 1 mm diameter beam of 2 MeV He^+ ions using silicon surface barrier detectors at scattering angles of 140° and close to 180° with an energy resolution of 13 keV and 18 keV, respectively. Angular scans across the $\langle 10\bar{1}1 \rangle$ axis along the $(1\bar{2}10)$ plane and across the $\langle \bar{2}113 \rangle$ axis along the $(10\bar{1}0)$ plane were performed with a two-axes goniometer with an accuracy of 0.01°. Simulations of ion channeling with the program package FLUX [11] were used to fit the angular scans. During the simulation of 10^5 ion trajectories, the average close-encounter probability is determined as a function of depth. This is repeated for a series of orientations of crystal axis and beam in steps of 0.1°. The simulated scan is derived directly from the orientation dependence of the close-encounter probability using the same depth windows as in the experimental spectra. In the calculations, vibration amplitudes u_2 of 0.08 Å, 0.14 Å, and 0.09 Å for Al, In, and N in AlInN, and 0.1 Å and 0.11 Å for Ga and N in GaN, respectively, were used. These are the published values for AlN [12] and GaN [13] while no data for InN were found in the literature. The value $u_2 = 0.14$ Å for In, resulting from a best fit to the experimental data, is very high when compared to the value for Ga, hinting at a static displacement rather than the consequences of dynamic lattice vibration. XRD reciprocal space maps (RSM) around the $(10\bar{1}5)$ reflections were acquired with a high resolution diffractometer equipped with a Göbel mirror, a 2-bounce Ge(444) monochromator and a position sensitive detector using Cu $K_{\alpha 1}$ radiation and a

beam size of $0.1 \times 4 \text{ mm}^2$. RSMs around an asymmetric reflection like $(10\bar{1}5)$ allow the determination of both the out of plane (c) and in-plane (a) lattice constants and hence a determination of lattice strain to compare with RBS/C values.

Figure 2 shows the random and $\langle 0001 \rangle$ aligned RBS/C spectra of sample S840. Fits to the random RBS spectra were performed with the NDF code [14]. Minimum yield values of 4%–6% for In reveal a good single crystalline quality, although they are slightly higher than for the GaN-buffer layer ($\sim 2\%$). The InN contents derived from the RBS/C spectra are summarized in Table I; as expected, they increase with decreasing growth temperature. The In distribution was found to be homogeneous throughout the layers' depth. Figure 3 shows the experimental and simulated $\langle \bar{2}113 \rangle$ Ga- and In-angular scans for sample S840. The energy windows used for In in the AlInN film and for Ga in the GaN-buffer layer are indicated in Fig. 2. A distortion of the channeling dip for Ga is observed, resulting in a second minimum at the same angular position as the minimum of the In scan. This distortion is due to the steering effects in the interface described above and is stronger for the samples with higher InN contents due to the smaller kink angles $\Delta\theta$. The distortion also influences the position of the minimum for the Ga scan and gives rise to a systematic error when strain values are determined directly from the displacement of the angular scans. MC simulations reproduce these steering effects accurately and allow a determination of $\Delta\theta$ from the fit to the experimental data. The values differ significantly from those derived directly from the shift of the scans (Table I). Steering effects decrease for higher beam energy, since the critical angle is proportional to $E^{-0.5}$. Angular scans measured for several energies between 0.5 and 2 MeV could be fitted with the same value of $\Delta\theta$. Simulations show further that steering effects become negligible only for energies as high as 8 MeV.
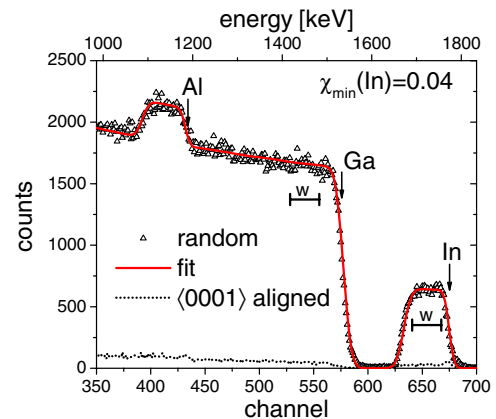

FIG. 2 (color online).   RBS/C random and $\langle 0001 \rangle$-aligned spectra taken with a 2 MeV He^+ beam for sample S840 and the fit to the random spectrum. Also indicated are the windows (w) used for the angular scans.

XRD RSMs (not shown) suggest that all of the ~100 nm films grow pseudomorphically on GaN. Uniquely for sample S800, grazing incidence diffraction (GID) measurements revealed a relaxation within a very thin surface layer, with an a lattice constant of 3.195 Å [15] not visible in the RSM and probably due to surface roughening. The lattice parameters a and c for the AlInN films, obtained directly from the RSMs, are summarized in Table I. With these and the lattice parameters for relaxed material (a_{rel} and c_{rel}) derived from Vegard's law, the tetragonal distortion can be calculated from XRD measurements: $\varepsilon_T = \varepsilon^{\parallel} - \varepsilon^{\perp}$ with $\varepsilon^{\parallel} = (a - a_{rel})/a_{rel}$ and $\varepsilon^{\perp} = (c - c_{rel})/c_{rel}$.

Note that values for ε_T, calculated either from RBS/C or XRD data, depend on the use of Vegard's law to determine the lattice parameters of relaxed AlInN. While we find excellent agreement between RBS/C and XRD measurements of strain, this is not the case for the determination of the InN contents. RBS allows the InN content to be measured directly, without assumptions about material properties. The InN contents determined from the XRD measurements using elasticity theory and the classical Vegard's law [as successfully applied to InGaN [16]] are overestimated in all three samples by $\sim6\%$ (i.e., about 1% in the absolute InN content) as compared to RBS (see Table I). Furthermore, the experimentally determined value of InN content for which lattice matching occurs ($\varepsilon_{\parallel} = 0$ for $x \sim 0.148$; $\varepsilon_T = 0$ for $x \sim 0.163$) does not agree with the prediction of Vegard's law ($x \sim 0.174$).

These discrepancies suggest that AlInN alloy, grown epitaxially on GaN, does not follow Vegard's law exactly. A real failure to obey Vegard's law can be caused by the large difference in size of the In and Al atoms and an apparent deviation by contaminations or minority phase inclusions, difficult to detect by XRD, but possibly affecting the composition measured by RBS. Nonideal behavior is common in compounds with large immiscibility regions like AlInN. Indeed, the elevated minimum yield and the large value for the apparent vibration amplitude for In mentioned above may indicate that a significant fraction of In atoms is not incorporated on perfect substitutional sites. A deviation from Vegard's law was also predicted by theory for wurtzite phase AlInN giving deviation parameters of 0.063 and -0.160 for the a and c lattice constant, respectively [17]. Several pairs of correction factors [in-
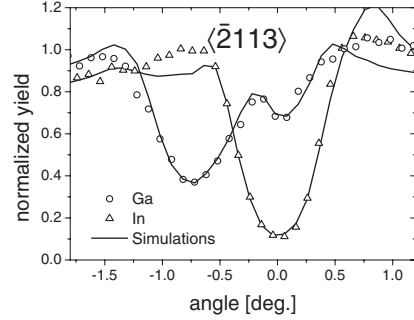
FIG. 3. Experimental angular scans for Ga and In across the $\langle\bar{2}113\rangle$ axis of sample S840 taken with a 2 MeV He$^+$ beam and Monte Carlo simulations.

cluding the ones from Ref. [17]] can reconcile the XRD and RBS/C data. However, using the factors from Ref. [17] lattice matching would be expected for InN contents of $\sim20\%$. This would mean that sample S800 is under slight tensile strain, contradicting the relaxation behavior seen in GID. Assuming that the a parameter measured by GID is the value for relaxed material for the corresponding InN content, the correction factors that reconcile all our data are -0.01 and -0.075 for the a and c lattice constants, respectively. ε_T calculated from RBS/C and XRD data using this nonlinear expression is presented in Fig. 4. The values of ε_T obtained by RBS/C in combination with MC simulations agree very well with the XRD results. However, it is clear that the use of the uncorrected values, derived directly from the shift of the channeling scans, would grossly overestimate ε_T.

The sign of the strain changes from tensile to compressive when the InN content of the layer is increased through the matching value [about 17.1(9)% in this determination], in very good agreement with the value predicted by the corrected Vegard's law (17%). Furthermore, the discrepancy between InN contents determined by RBS and XRD could be eliminated (see Table I). However, we must note that the determination of the InN fraction by XRD depends also on the choice of values for the lattice parameters and the elastic constants of AlN and InN. The values used in this study are $a = 3.111$ Å, $c = 4.98$ Å [18], $c_{13} = 99$, $c_{33} = 389$ [19] for AlN and $a = 3.53774$ Å, $c = 5.7037$ Å [20], $c_{13} = 121$, $c_{33} = 182$ [21] for InN. The literature values

TABLE I. InN contents measured by RBS, InN contents measured by XRD using the classical (cl) and corrected (corr) Vegard's law, AlInN lattice parameters, and the kink angles $\Delta\theta$ in the interface for measurements with 2 MeV α particles for the $\langle10\bar{1}1\rangle$ and the $\langle\bar{2}113\rangle$ axes, determined from the fit and read directly from the displacement of the scans.

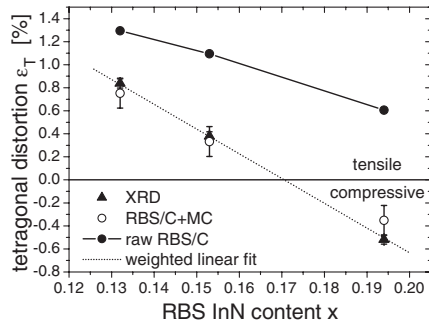| Sample	InN% RBS	InN% XRD (cl)	InN% XRD (corr)	a [Å]	c [Å]	$\Delta\theta \langle10\bar{1}1\rangle$ fit	$\Delta\theta \langle10\bar{1}1\rangle$ scan	$\Delta\theta \langle\bar{2}113\rangle$ fit	$\Delta\theta \langle\bar{2}113\rangle$ scan
S800	19.4(5)	20.6(1.0)	19.4(1.0)	3.185(1)	5.142(1)	0.31(5)°	0.58(5)°	0.26(5)°	0.51(5)°
S820	15.3(5)	16.2(1.0)	15.3(1.0)	3.185(1)	5.093(1)	0.51(5)°	0.70(5)°	0.46(5)°	0.68(5)°
S840	13.2(5)	14.0(1.0)	13.1(1.0)	3.185(1)	5.068(1)	0.66(5)°	0.77(5)°	0.56(5)°	0.74(5)°

FIG. 4. The tetragonal distortion ε_T measured by RBS/C and XRD as a function of the InN content measured by RBS and the weighted linear fit to all the data. The values for "raw RBS/C" were determined directly from the minima of the angular scans; the "RBS/C + MC" values were derived with help of a fit to the experimental data using Monte Carlo simulations.

for InN scatter significantly, leading to the large estimated error for the XRD InN content. We cannot rule out the possibility that insufficient accuracy in material parameters or undetected minority phases are responsible for the discrepancy in composition evidenced between RBS and XRD measurements.

Further investigation of the validity of Vegard's law needs to be performed on samples with a wider range of InN fractions and the issue of minority phases has to be addressed in more detail.

In summary, near-lattice-matched AlInN/GaN bilayers grown by MOCVD in the temperature range from 800 to 840 °C show good crystalline quality as well as a homogeneous InN distribution. Steering effects in the interface influence the angular yield from the GaN-layer in RBS/C and cause failure of the conventional means of assessing strain by RBS/C. We have shown for the first time that MC simulations are viable as a routine tool to correct channeling results for such steering effects, leading to an excellent agreement of RBS/C and XRD strain measurements. Furthermore, we demonstrate the importance of an absolute measurement of the InN content by RBS/C when the accuracy of XRD composition determination in AlInN is limited due to suspected deviations from Vegard's law and/ or uncertainty regarding the real values of material parameters. Our results give an indirect confirmation of the theoretically predicted deviation from Vegard's law and possible correction factors were estimated. Following these corrections and the experimental results, lattice matching is predicted to occur at an InN content of 17.1(9)%.

*Corresponding author.
Current address: Departamento de Física, ITN, Estrada Nacional 10, 2686-953 Sacavém, Portugal.
Tel.: +351-994-6056
Fax: +351-994-1525
Email address: lorenz@itn.pt

[1] *Group III Nitride Semiconductor Compounds, Physics and Applications*, edited by B. Gil, Series on Semiconductor Science and Technology 6 (Oxford Science Publications, Oxford, 1998).
[2] J. F. Carlin, C. Zellweger, J. Dorsaz, S. Nicolay, G. Christmann, E. Feltin, R. Butte, and N. Grandjean, Phys. Status Solidi B **242**, 2326 (2005).
[3] A. Dadgar, F. Schulze, J. Bläsing, A. Diez, A. Krost, M. Neuburger, E. Kohn, I. Daumiller, and M. Kunze, Appl. Phys. Lett. **85**, 5400 (2004).
[4] I. M. Watson, C. Liu, E. Gu, M. D. Dawson, P. R. Edwards, and R. W. Martin, Appl. Phys. Lett. **87**, 151901 (2005).
[5] S. T. Picraux, W. K. Chu, W. R. Allen, and J. A. Ellison, Nucl. Instrum. Methods Phys. Res., Sect. B **15**, 306 (1986).
[6] E. Alves, S. Pereira, M. R. Correia, E. Pereira, A. D. Sequeira, and N. Franco, Nucl. Instrum. Methods Phys. Res., Sect. B **190**, 560 (2002).
[7] L. C. Feldman, J. W. Mayer, and S. T. Picraux, *Materials Analysis by Ion Channeling* (Academic, New York, 1982).
[8] L. Vegard, Z. Phys. **5**, 17 (1921).
[9] C. Wu, S. Yin, J. Zhang, G. Xiao, J. Liu, and P. Zhu, J. Appl. Phys. **68**, 2100 (1990).
[10] S. Hernandez, K. Wang, D. Amabile, E. Nogales, D. Pastor, R. Cusco, L. Artus, R. W. Martin, K. P. O'Donnell, and I. M. Watson, MRS Symposia Proceedings No. 892 (Materials Research Society, Pittsburgh, 2005), paper FF 23.4.
[11] P. J. M. Smulders and D. O. Boerma, Nucl. Instrum. Methods Phys. Res., Sect. B **29**, 471 (1987).
[12] E. Gabe, Y. Le Page, and S. L. Mair, Phys. Rev. B **24**, 5634 (1981).
[13] A. Yoshiasa, K. Koto, H. Maeda, and T. Ishii, Jpn. J. Appl. Phys. **36**, 781 (1997).
[14] N. P. Barradas, C. Jeynes, and R. P. Webb, Appl. Phys. Lett. **71**, 291 (1997).
[15] J. Bläsing and A. Krost, University of Magdeburg (private communication).
[16] S. Pereira, M. R. Correia, T. Monteiro, E. Pereira, E. Alves, A. D. Sequeira, and N. Franco, Appl. Phys. Lett. **78**, 2137 (2001).
[17] B. T. Liou, S. H. Yen, and Y. K. Kuo, Appl. Phys. A **81**, 651 (2005).
[18] M. Tanaka, S. Nakahata, K. Sogabe, H. Nakata, and M. Tabioka, Jpn. J. Appl. Phys. **36**, L1062 (1997).
[19] W. Paszkowicz, R. Cerny, and S. Krukowski, Powder Diffr. **18**, 114 (2003).
[20] L. E. McNeil, M. Grimsditch, and R. H. French, J. Am. Ceram. Soc. **76**, 1132 (1993).
[21] A. F. Wright, J. Appl. Phys. **82**, 2833 (1997).